Progress in Natural Science: Materials International 2013;23(3):273–285

Chinese Materials Research Society

Progress in Natural Science: Materials International

www.elsevier.com/locate/pnsmi
www.sciencedirect.com

REVIEW

# Recent advances in multistep solution nanosynthesis of nanostructured three-dimensional complexes of semiconductive materials

**Huajun Zhou**[a,b], **Z. Ryan Tian**[a,b,*]

[a]*Department of Chemistry and Biochemistry, University of Arkansas, Fayetteville, AR 72701, USA*
[b]*Institute of Nanoscale Materials Sciences and Engineering, University of Arkansas, Fayetteville, AR 72701, USA*

Received 10 September 2012; accepted 10 March 2013
Available online 15 June 2013

**KEYWORDS**

Three dimensional;
Complex structures;
Semiconductor;
Multistep;
Solution synthesis

**Abstract** Constructing simply nanostructured zero-, one-, and two-dimensional crystallites into three-dimensional multifunctional assemblies and systems at low-cost is essential and highly challenging in materials science and engineering. Compared to the simply nanostructured components, a three-dimensional (3D) complex made with a precisely controlled spatial organization of all structural nanocomponents can enable us to concert functionalities from all the nanocomponents. Methodologically, so doing in nm-scales via a solution chemistry route may be much easier and less expensive than via other mechanisms. Hence, we discuss herein some recent advances in multistep solution syntheses of nanostructured 3D complexes of semiconductors with a focus mainly on their synthetic strategies and detailed mechanisms.



## 1. Introduction

During the past a few decades, nanostructured inorganic semiconductors with a wide range of structural complexities have been extensively researched. This is mainly because of their tunable chemical/physical properties that are potentially useful in a wide range of important applications, e.g. nanolasing [1], electronics [2], optoelectronics [3], catalysis [4], solar cells [5], sensing [6], separation [7], etc. In comparison with 0D, 1D, and 2D micro/nanostructures, nanostructured 3D complexes often provide us

*Corresponding author at: Department of Chemistry and Biochemistry, University of Arkansas, Fayetteville, Arkansas 72701, USA. Tel.: +1 479 575 2653; fax: +1 479 575 4049.
E-mail address: rtian@uark.edu (Z. Ryan Tian).

Peer review under responsibility of Chinese Materials Research Society.

Production and hosting by Elsevier

1002-0071 
http://dx.doi.org/10.1016/j.pnsc.2013.05.005

with improved or even new functionalities [8,9] due to their unique complexity in shape, organization, and orientation of their nanocomponents [10,11]. Firstly, 3D topology really matters in applied nanoscience. One outstanding example is the use of inverted pyramid texturing geometry for trapping light effectively [12] in high-efficiency Si solar cells [13]. Hybrid solar cells based on CdSe nanotetrapods, as another great example, have demonstrated a higher external quantum efficiency (EQE) than that based on CdSe nanorods [14], due to the extensive intra-crystallite light scattering and thus-enhanced light absorption of the interpenetrating nanotetrapod networks [15]. Under this inspiration, one should be able to build in theory, much freely by design, a long list of low-cost multifunctional assemblies and even systems that can spatially concert functionalities of all the nanocomponents [16,17]. This indeed calls for new total nanosyntheses specifically good for making future multifunctional crystallites with structural complexities too high to be realized at low cost by other means, e.g. 3D nanomachining or nanoprinting. In order to materialize a structure- or function-oriented design, a total nanosynthesis may need to alternate the use of techniques for mimicking the addition, protection, and elimination that are routinely used in a typical organic total synthesis.

Compared to high temperature solid-state synthetic methods such as chemical vapor deposition (CVD) [18], physical vapor deposition (PVD) [19,20], and vapor–liquid–solid (VLS) growths [21], solution synthesis offers two main advantages: (1) the relatively mild reaction conditions allow for easy operation and wider choices of substrates; (2) reactions could be scaled up easily at low cost. In literature, multistep solution syntheses of novel types of nanostructured 3D complexes via a variety of ways have been reported in a rather sporadic manner. Here, our discussion will focus on the nanostructured 3D complexes formed in a stepwise fashion from solution routes, especially those easy to control and scale up in potential industrial production. The stepwise syntheses occurred either in consecutive reaction steps or in a one-pot process. Hence, the discussion will cover those complex structures grown under the help of templates and other methods such as micropatterning, photolithography, and Langmuir–Blodgett (LB) thin-film fabrication. In parallel, complex structures consisting of both semiconductor and non-semiconductor components will be included in the discussion. Although heterojunctions are fundamentally different from homojunctions and have been widely studied and integrated into devices for real applications [22], our emphasis will be put more on their formation mechanisms than on their structure-related functionalities due to the limit of space here. However, even within the narrow scope of the above-mentioned focuses, it is still far from being possible to cover all important works published in this fast progressing field in the relative short discussion below.

## 2. Nanostructured 3D complexes grown on 0D nanocores: from multipods to flower-like structures and spheres

Hierarchical structures are classified according to the dimensionalities of building units and the consecutive hierarchical structures [23,24]. However, nanostructured 3D complexes could consist of multi-nanocomponents with different dimensionalities, the 3D complex structures reviewed here will be classified by differentiating the different combinations of nanocomponents with different dimensionalities, the orders of topological complexity of the final structures, and the methods employed in their syntheses. In this section, we will discuss those structures grown on 0D nanocore materials that could be nuclei, polyhedrons, cubes, or spheres. As the densities of subsequently grown 1D nanowires or nanorods increase, the final morphologies evolve from multipods, to flower-like structures, and then to spheres.

Fig. 1a illustrates the stepwise formation and TEM image of CdTe nanotetrapods [10,11]. Firstly, tetrahedral nuclei of zinc blende phase formed. Due to the identical nature of the (111) facets of zinc blende phase and $(000\bar{1})$ facets of wurtzite phase, subsequent epitaxial growth of CdTe legs of wurtzite phase on four $(000\bar{1})$ facets led to the formation of CdTe nanotetrapods. This mechanism also applies to the formation of other tetrapods and branched structures [25]. Under other conditions, pyramid nuclei of wurtzite phase form first. These nuclei then aggregate through multiple wurtzite twinning to form bigger nuclei of different shapes from which further multiple wurtzite twinning leads to the formation of CdTe bipods, tripods, and tetrapods [26]. Similar crystal growths driven by multiple crystal twinning apply to the formation of MnS bipod, tripod, and tetrapod [27] and branched $Cu_2O$ nanoparticles [28]. Formation of nuclei followed by growths of branches on nuclei to afford multipods is quite common, as further proven by the syntheses of ε-$MnO_2$ nanostructures with three to six branches grown on nuclei formed in situ depending on reaction parameters [29]. In all of them, the crystal habits and reaction conditions play determining roles in shaping nuclei and directing the subsequent branch growths.

In order to prepare structures with novel morphologies, bigger 0D nano/microparticle with designed structures and chemical compositions are grown first and then used as cores to support further branch growths. Fig. 1b illustrates the growth of ZnO nanorods on Ag truncated nanocubes [30]. Ag truncated nanocubes were prepared first and then immersed in hydrothermal reactions between $Zn(NO_3)_2$ and hexamethylenetetramine (HMT) for ZnO branch growth. Each Ag truncated nanocube (∼ 150 nm in diameter) consists of eight {111} facets and six {100} facets and all four ZnO nanorods were selectively grown on {111} facets due to the good lattice match and symmetry match between the corresponding planes of ZnO and Ag, and the direct interfacing of the Zn layer with Ag that could initiate the formation of the ZnO lattice. The use of metal nanoparticles as nanocores to graft semiconductor nanowires/rods also applies to the syntheses of multipods of Au–, Ag–, and Pd–PbSe [31], etc. As another example, cuboctahedral $Cu_{2-x}Se$ (10–15 nm in diameter) nanocrystals of cubic berzelianite phase were firstly prepared [32] and injected into reactions of preparing CdS nanoparticles [33]. The $Cu_{2-x}Se$ seeds underwent cation exchanges to form cubic sphalerite CdSe seeds that inherited the original cuboctahedral shapes. Fast growth along eight {111} facets of each cuboctahedral CdSe seed led to the formation of octapods with CdSe core and eight CdS legs.

For all the multipods discussed in the above, the nanocores onto which branches were grown are crystalline. Fig. 1c illustrates the use of amorphous $SiO_2$ microspheres as cores for further grafting of ZnO microrods. $SiO_2$ microspheres were prepared first [34] and immersed into hydrothermal reactions between $Zn(NO_3)_2$ and HMT [35]. Different numbers of ZnO microrods could be grafted onto each microsphere and the SEM image of a decapod is shown in Fig. 1c (right). The surface of $SiO_2$ microspheres could be largely covered by either Si–OH or Si–O–Si groups [36] both of which could coordinate to $Zn^{2+}$ cations in the solutions. The coordinated $Zn^{2+}$ ions then reacted with $OH^-$ groups that were released from the hydrolysis of HMT, leading to the formation of ZnO microrods on

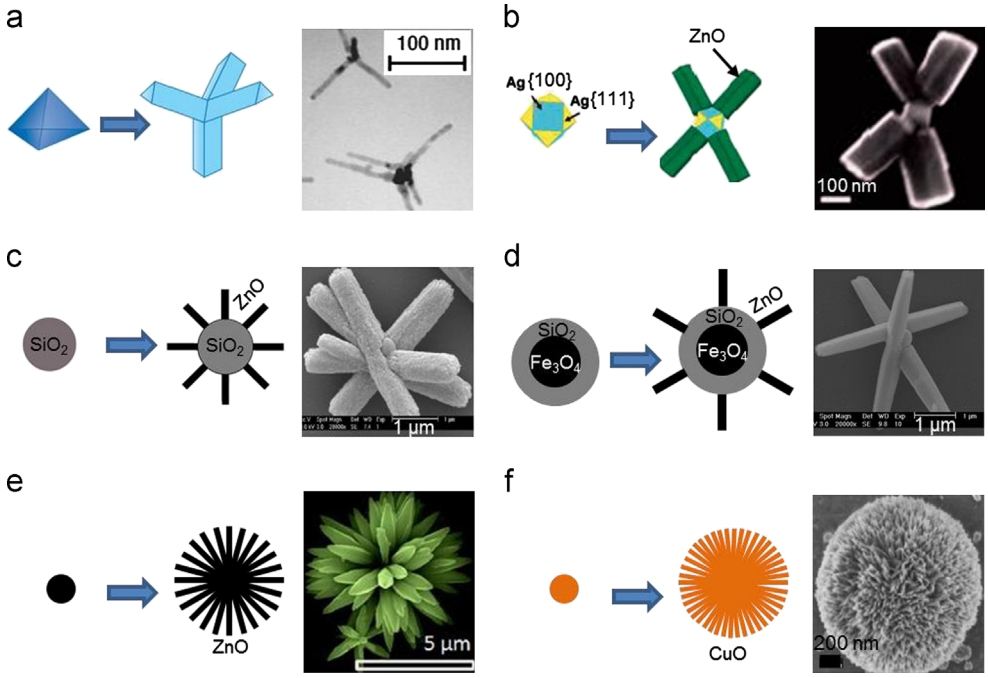


**Fig. 1** 3D complex structures grown on 0D cores: from multipods, to flower-like structures, and to spheres. Schematic representations of the formation and TEM image of CdTe tetrapods (a), SEM images of the heterostructure of four ZnO nanorods on Ag truncated nanocubes (b), the heterostructure of a few ZnO nanorods on $SiO_2$ microspheres (c), a hexapod with ZnO microrods on $Fe_3O_4$@$SiO_2$ microsphere (d), flower-like ZnO microstructure (e), and urchin-like CuO microstructures (f). (a) Reproduced with permission from Nature Mater. 2 (2003) 355–356 and Nature Mater. 2 (2003) 382–385; (b) from J. Am. Chem. Soc. 131(34) (2009) 12036–12037; (c) from Smart Mater. Struct. 15(2) (2006) N46–N50; (e) from Proc. Natl. Acad. Sci. U.S.A. 107(31) (2010) 13588–13592; (f) from Mater. Res. Bull. 43(3) (2008) 771–775.

$SiO_2$ microspheres. To bring more functionalities (e.g. magnetism) into "spiky" structures as prepared above, we recently succeeded in grafting ZnO microrods onto the surface of $Fe_3O_4$@$SiO_2$ core–shell microspheres (Fig. 1d). $Fe_3O_4$ microspheres with permanent magnetism were prepared first [37] and then coated with $SiO_2$ shell through modified Stöber process [38]. Then the resulting $Fe_3O_4$@-$SiO_2$ core–shell microspheres were immersed into similar hydrothermal reactions between $Zn(NO_3)_2$ and HMT for grafting ZnO microrods. It is also believed that the Si–OH or Si–O–Si groups on $SiO_2$ shells attribute to the nucleation and further growth of ZnO microrods. In many cases, many 1D nanowires or nanorods were grown on 0D nanocores, which could be nuclei or as-grown spheres or polyhedrons, to form flower-like structures. Fig. 1e illustrates the formation of the flower-like assembly of Al-doped (2–3.5%) ZnO microrods [39]. A solution containing $Zn(CH_3COO)_2$, $Al(NO_3)_3$, and NaOH in mixed solvent of water/ethanol (1/1) was sonicated first and then transferred to a Teflon-line autoclave for solvothermal synthesis. Cores first nucleated out and ZnO nanorods were grown on them from many directions. The nature of the inside core is not well understood yet. Such kinds of flower-like semiconductor assemblies include binary compounds such as $TiO_2$ [40], $Fe_2O_3$ [41], $SnO_2$ [42,43], ZnO [44], CdS [45,46] CdSe [46,47], and tertiary compounds such as $PbTiO_3$ [48], β-$AgVO_3$ [49] In addition to the use of 1D nanowires or nanorods as the building units, 2D structures such as nanoplates/sheets could be grown on nuclei from many directions to form flower-like structures [50]. As-grown 0D structures either crystalline or amorphous could be used as nanocores to grow many branches to afford flower-like structures such as Au–CdSe and Ag–CdSe [51], $SiO_2$–ZnO [35]. There are some flower-like structures, either similar to or different from the flower-like structures discussed here, the formation mechanisms of which are not completely understood yet [52].

Sphere-like structures would be obtained if branches were grown at all directions. Fig. 1f illustrates the formation of CuO urchin-like nanostructures that were prepared via a hydrothermal microwave route using polyethyleneglycol (PEG), $Cu^{2+}$ ion, and $NH_4OH$ as starting materails [53]. Firstly, the reaction between $Cu^{2+}$ ion and $NH_4OH$ in the presence of PEG led to the formation of initial nuclei that were adsorbed by PEG through $OH^-$ groups. The resulting particles served as cores onto which CuO NWs were grown at all directions to afford CuO urchin-nanostructures. The mechanism applies to the formation of other microspheres [54] and hemispheres [55] with the help of self-assembly processes in some cases. This kind of sphere-like heterostructures could also be made by grafting 1D nanowires/nanorods from all directions onto preexistent spheres of same or different chemical compositions such as γ-$Fe_2O_3$@$SiO_2$ core–shell [56], polystyrene [57], Zn [58], ZnO [59], $Al_2O_3$ [59], etc.

## 3. Nanostructured 3D complexes grown on 1D-, 2D- and 3D-nanostructures

1D nanostructures (rods, wires, and tubes) have been the most widely used building units of 3D complexes and they could be used as backbones or branches grown on other backbones. Fig. 2a shows the scheme of growing 1D branches onto 1D backbones. Fig. 2b shows the SEM image of an array of the carbon-nanotubes (CNTs)-ZnO heterostructure in which each CNT is covered by densely packed ZnO nanowire arrays (inset in Fig. 2b) [60].

Vertical array of CNTs was firstly deposited on a small Ta plate [61] and then coated with a thin film of ZnO by radiofrequency sputtering coating. Subsequent hydrothermal reaction in a solution saturated with $Zn(OH)_4^{2-}$ led to the grafting of densely packed ZnO nanowires onto each CNT. The coated ZnO film attributes to the nucleation and further growth of dense ZnO nanowires. Other nanowires such as CdSe nanowires were also grown onto CNTs [62] and 1D structures were could be grafted onto other nanotubes such as α-$Fe_2O_3$ nanotube [63] and ZnO microtube [64].

Semiconductors of 1D nanowires or nanorods such as Si [65–67], ZnO [68–70], $TiO_2$ [71–76], $SnO_2$ [77], $Fe_2O_3$ [78], WOx [79,80], have been widely used as backbones onto which 1D or 2D structures of same or different chemical compositions have been grafted. Fig. 2c shows the SEM image of a structure composed of a ZnO microrod with secondary branches. ZnO microrods with well-defined hexagonal crystallographic planes were first deposited onto a glass substrate when a substrate cleaned with wet chem wipes was put into a vial containing $Zn(NO_3)_2$ and HMT for hydrothermal reaction. Then the glass substrate with ZnO microrods was immersed into an aqueous solution containing $Zn^{2+}$ ions and certain concentration of diaminopropane at 60 °C for a few hours. Diaminopropane could control branch nucleation and growth by affecting the ZnO solubility through the formation of Zn-diaminopropane complexes and pH [81]. Each of six side surfaces is entirely covered by layers of ZnO nanorods [82]. The densities, diameters, and lengths of the nanorods could be tuned by controlling the concentration of diaminopropane and reaction time. Actually, similar branch growth patterns but with less densely packed branches were also prepared. The coverage of branched materials on backbone structures could be affected by other factors such as densities of pre-deposited seeds [83], their lattice mismatch [74], reaction parameters, etc.

In addition, metal nanowires or nanorods could also be used as backbones to grow semiconductor nanobranches [84] or grown onto semiconductor nanowires [83]. Besides the above-discussed widely studied semiconductors, 1D nanowires or nanorods of other semiconductors were also employed to build 3D complexes [85]. Fig. 2d shows the heterostructures of $MnMoO_4$ nanowires with $CoMoO_4$ nanobranches. $MnMoO_4$ nanowires were prepared first and then $CoMoO_4$ nanobranches were grafted through self-assembly and "oriented attachment" mechanism [86]. $CoMoO_4$ nanoparticles with high surface energy and thermodynamics instability linked to adjacent particles so that they had the same crystallographic orientation. $CoMoO_4$ nanoparticles could also attach to the surface of $MnMoO_4$ nanowires to further decrease surface energy due to their good lattice match. For the same reason, the lattice fringe's orientation of $CoMoO_4$ nanoparticles and the direction of further crystal growth onto $MnMoO_4$ nanowires were uniform to some extent. 1D semiconductor nanowires were also grown on 1D structures of bigger dimensions even to macroscopic scales such as carbon fiber [87], Kevlar fibers [88], and optic fibers [89] to achieve specific functionalities.

On the basis of the above structures, further increasing the orders of topological complexity could result in the formation a family of structures called "dendrites" that are of great importance due to their functionalities and wide potential applications [90–94]. A dendrite refers to a structure that has a primary stem from which secondary, tertiary, or even higher order side branches grow out [95]. Dendrite micro/nanostructures of different semiconductors such as PbS [96], $Cu_2O$ [97], ZnSe [98], CdTe [47], α-$Fe_2O_3$ [99], γ-$Fe_2O_3$ [100], $Fe_3O_4$ [100], ZnO [101–104], and $TiO_2$ [105–107] were prepared in a controllable fashion. Snowflakes structures also belong to the family of dendrites [108]. Fig. 3a illustrates the stepwise formation of dendrite crystals of α-$Fe_2O_3$ that were obtained by heating aqueous solution of $K_3[Fe(CN)_6]$ of a certain concentration in a Teflon-sealed autoclave at suitable temperatures for 2 days [108]. The slow dissociation of $Fe^{3+}$ ions from $[Fe(CN)_6]^{3-}$ ions under hydrothermal conditions played a vital role in the crystal growth process. The growth along $[1\bar{1}00]$ was much faster than all the other directions, resulting in the formation of needles. Subsequent growth along two crystallographically equivalent directions (i.e. $[10\bar{1}0]$ and $[0\bar{1}10]$) led to the formation of secondary branches on both sides of each needle. As crystal growth continued, tertiary branches could grow on secondary branches and quaternary branches on tertiary branches. In the whole growth process, the stem and branches at all orders became thicker and longer and eventually interconnected with each other to form the micro-pine dendrite structures. There are also some dendrites [109–110], the formation mechanisms of which need further exploration.

In the formation of above-discussed complex structures grown on 1D backbones, branching from the sides of trunks and higher order branches dominates. Milliron et al. demonstrated the selective branching from two ends of a nanorod or four tips of a nanotetrapod (Fig. 4) [25]. Starting CdSe nanorods (Fig. 4a) were prepared and Te dissolved in tri(n-alkylphosphine) were added to solutions containing CdSe nanorods to induce further growth of CdTe in the presence of excessive Cd species. Wurtzite CdTe could nucleate at one end of a CdSe nanorod, assisting the linear extension of CdTe nanorod at one end. Simultaneously, zinc blende CdTe could

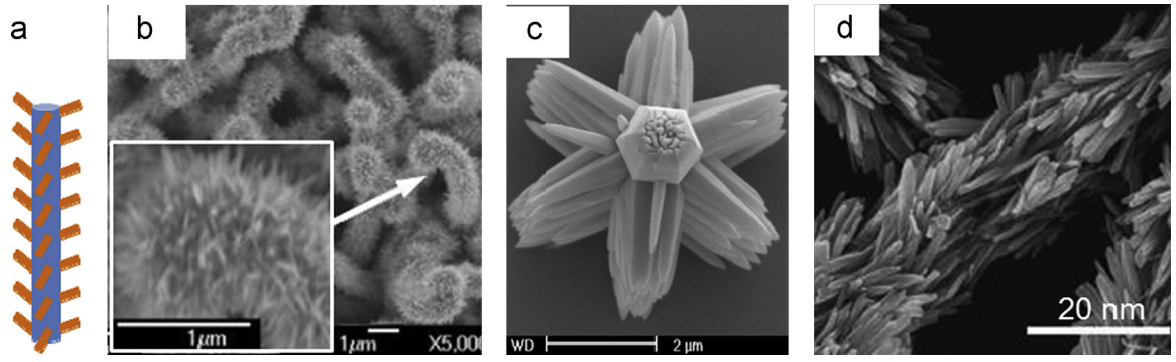


**Fig. 2** 3D complex structures composed of 1D structures (tube, rod, wire) grown on 1D backbones. (a) Schematic representation of the structures; (b) SEM of an array of ZnO nanowires on CNTs (inset is the SEM image of ZnO nanowires on one CNT at higher magnification); (c) a ZnO microrod with ZnO secondary nanobranches; (d) $CoMoO_4$ nanobranches on $MnMoO_4$ nanowires (d). (b) Reproduced from Nanotechnology 17(4) (2006) 1036–1040; (c) from J. Am. Chem. Soc. 128(33) (2006) 10960–10968; (d) from Nature Commun. 2 (2012) 381.

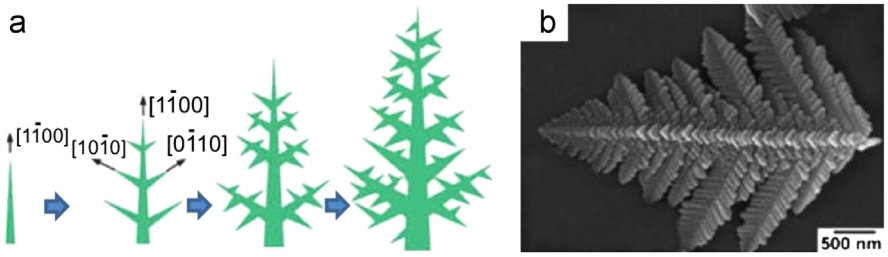


**Fig. 3** (a) Schematic representation of the formation process and (b) SEM image of fractal dendrite crystals of α-$Fe_2O_3$. Reproduced with permission from Angew. Chem. Int. Ed. 44(27) (2005) 4197–4201.

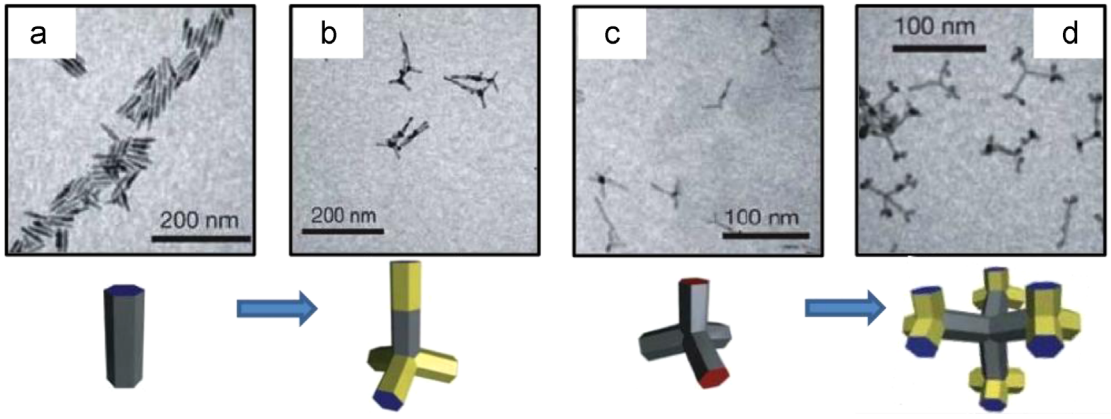


**Fig. 4** 3D complex nanostructures formed by selective branching from two ends of each nanorod or four tips of each nanotetrapod. (a) The starting CdSe nanorods; (b) branched rods resulting from nucleation of CdTe on both ends of CdSe nanorod. A CdTe zincblende region at one end creates the branch point; (c) the starting CdSe nanotetrapods; (d) branched tetrapods resulting from nucleation of CdTe zincblende branch points on tips of nanotetrapods. Reproduced with permission from Nature 2004, 430, 190–195.

nucleate at the other end of the CdSe nanorod, thus inducing the growth of CdTe tripod at the other end (Fig. 4b). Similarly, starting CdSe nanotetrapods (Fig. 4c) were prepared first, which was followed by selective nucleation of zinc blende CdTe on all the tips of CdSe nanotetrapods. Sequential growth of wurtzite CdTe induced growth of CdTe tripods at tips of CdSe nanotetrapods (Fig. 4d). This mechanism also applies to formation of highly branched Labyrinthine-shaped CdSe nanostructures [111].

Structures of higher dimensionalities such as 2D nanoplates or nanosheets could also be deposited onto 1D backbones [68,72,73,85]. Besides 1D structures, 2D structures [112–115], such as discs and plates were also used as supports to grow 3D complex structures. Fig. 5a illustrates the stepwise growth of α-$Fe_2O_3$–$SnO_2$ nanocombs (Fig. 5c) by grafting $SnO_2$ nanorod arrays onto both sides of α-$Fe_2O_3$ nanoflakes (Fig. 5b) [115]. α-$Fe_2O_3$ nanoflakes were prepared first by annealing a cleaned Fe foil at 400 °C and then the substrate was immersed into aqueous solution $Na_2Sn(OH)_6$ for hydrothermal reactions. $SnO_2$ nanorods were grown on ($\pm$001) planes of $Fe_2O_3$ nanoflakes through epitaxial growth due to the good lattice match between the corresponding planes. 3D structures such as nanotetrapods [116] were also used as supports for further growth 3D complex structures.

## 4. Multistep syntheses of nanostructured 3D complexes with higher orders of topological complexity

In previous sections, we discussed nanostructured 3D complexes that were prepared in no more than two reaction steps even though their formations could take a few steps. In one case, nuclei form first and growths of complex structures from nuclei follow. In another case, 0D, 1D, 2D, and 3D starting structures are prepared first as nanocores or supporting materials for further growths of complex structures (in some cases, seeding on the starting structures is necessary for further growths). In order to make structures with higher orders of topological complexity, the method of "multistep ($n\geq3$) sequential nucleation and growth" has been employed and received considerable attention. Fig. 6a illustrates this strategy to prepare the micropatterned array of tertiary ZnO "cactus" structures through four growth stages on a micropatterned substrate [117]. The first step involved the creation of patterned nucleation sites on a Ag substrate through micropatterning, which was followed by growth of oriented nanorods from the nucleation sites. Subsequent growths of secondary branches from the primary nanorods and tertiary branches from the secondary branches led to the formation of patterned arrays of ZnO "cactus". Fig. 6b and c exemplify "engineering" the complex structures by tuning the orders of adding structure directing agents (SDAs) [82], which can greatly enrich the database of complex structures prepared through the "multistep sequential nucleation and growth" method. For the syntheses shown in Fig. 6b, ZnO microrods were first deposited onto a glass substrate and then the substrate with microrods was immersed into an aqueous solution of $Zn^{2+}$ and diaminopropane to grow structures of microrods with secondary nanobranches. Diaminopropane directed both the nucleation and growth of secondary nanobranches [81]. Then the substrate was immersed into an aqueous solution of $Zn^{2+}$ and citrate ions for grafting tertiary nanoplates. Tertiary nanoplates

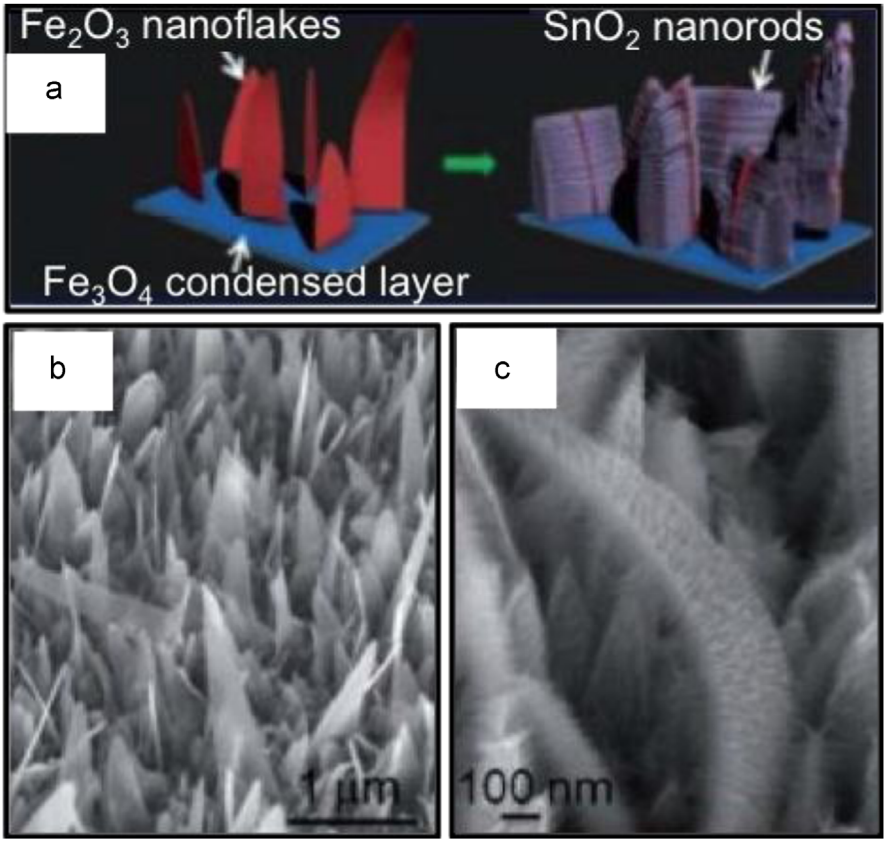


**Fig. 5** (a) Schematic representation of the formation of nanocomb-like heterostructure of $SnO_2$ nanorods on $Fe_2O_3$ nanoflakes; (b–c) SEM images of starting $Fe_2O_3$ nanoflakes (b) and nanocomb-like heterostructure of $SnO_2$-$Fe_2O_3$. (c). Reproduced with permission from Nanoscale 4(15) (2012) 4459–4463.

were grown onto both the primary microrod and the secondary nanobranches. Citrate ions tended to induce the growth of nanoplates [118] since citrate ions could preferentially adsorb onto the basal planes of ZnO [119] and thus inhibit the growths along {1000} directions. In contrast, when citrate ions were added in the secondary growth and DAP in the tertiary growth, both the secondary structures and the tertiary structures obtained (Fig. 6c) differ dramatically from those obtained in the previous case. The two kinds of 3D tertiary structures may barely find any analogs in nature. Multistep nucleation and growth have also proved successful in preparing many unprecedented structures such as wagon-wheel-like ZnO crystals and multilayered ZnO structure composed of alternating layers of ZnO microrods and microplates [117].

Beside crystal growth, selective dissolution could be integrated into the above-mentioned "multistep sequential nucleation and growth" method to further increase the complexity orders and diversity of 3D complexes. Fig. 7 exemplifies selective dissolution as a power method in preparing 3D complexes with novel morphologies [120]. CdSe nanotetrapods (Fig. 7b) were firstly prepared [121] and encapsulated with silica shells [122] to afford silica-coated CdSe nanotetrapods which were easily dispersible due to their unique morphologies and colloidally stable in aqueous solutions due to the silica coating. The inner silica shells were then removed by dilute HF with optimized concentration after proper etching time while the outer shells remained intact due to the inhomogeneous nature of silica shells since the outermost layers possess higher degrees of Si–O cross-linking and thus higher stability against etching [123]. Then Pt nanoparticles were decorated onto CdSe nanotetrapods, which would be impossible without removal of the inner silica shells since the intimate contact between CdS and the silica shells would inhibit nucleation and growths of Pt nanoparticles. Pt-nanoparticles-decorated CdSe nanotetrapods within hollow $SiO_2$ interiors, when exposed to $Ag^+$ or $Pd^{2+}$ solution for 1 h, underwent further cation exchange to afford Pt-nanoparticle-decorated $Ag_2S$ or PdS nanotetrapods within hollow $SiO_2$ interiors (Fig. 7b).

## 5. Nanostructured 3D complexes from templateless self-assemblies

Self-assembly of as-grown nanocomponents is another powerful method to grow nanostructured 3D complexes. Fig. 8a illustrates the schematic formation of a chain from self-assembly of CdSe octapods [124]. CdSe octapods (Fig. 8b) were prepared first following previous published procedure [33] and dispersed in toluene. Since the van der Waals attractions between octapods are slightly stronger than that between octapods and toluene, octapods then interlocked each other to form chains (Fig. 8c) within each of which each octapod is tilted by 45° with respect to its nearest neighbors (Fig. 8a). Addition of acetonitrile into a toluene solution of CdSe octapods boosted the attraction between octapods and between chains, thus guiding further assembly of chains into 3D micrometer-sized superstructures of octapods (Fig. 8d and e). This

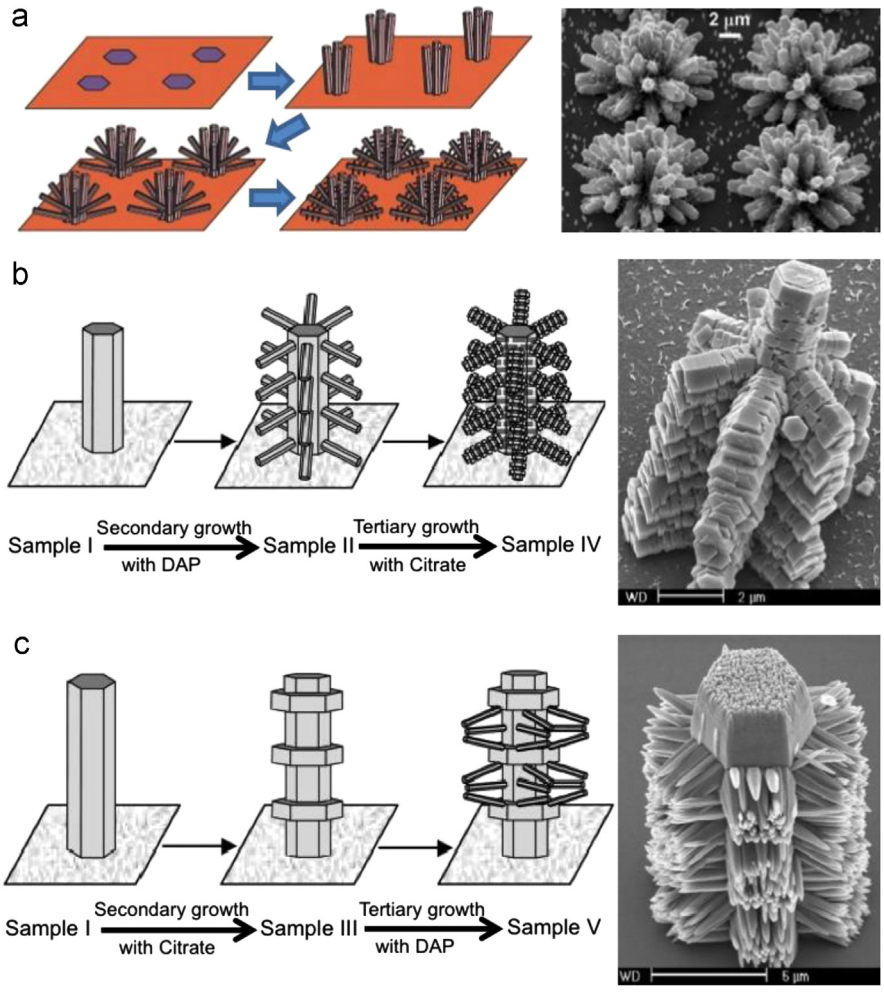


**Fig. 6** Three kinds of 3D complex structures prepared using the method of "multistep sequential nucleation and growth". (a) Scheme of the formation and SEM image of tertiary ZnO "cactus" structures; (b–c) Schematic representations of the formation and SEM images of two tertiary ZnO structures with novel morphologies by switching the orders of adding DAP and citrate as structure directing agents (SDAs) in secondary and tertiary growths. (a) Reproduced with permission from Adv. Funct. Mater. 16(3) (2006) 335–344; (b) and (c) from J. Am. Chem. Soc. 128(33) (2006) 10960–10968.

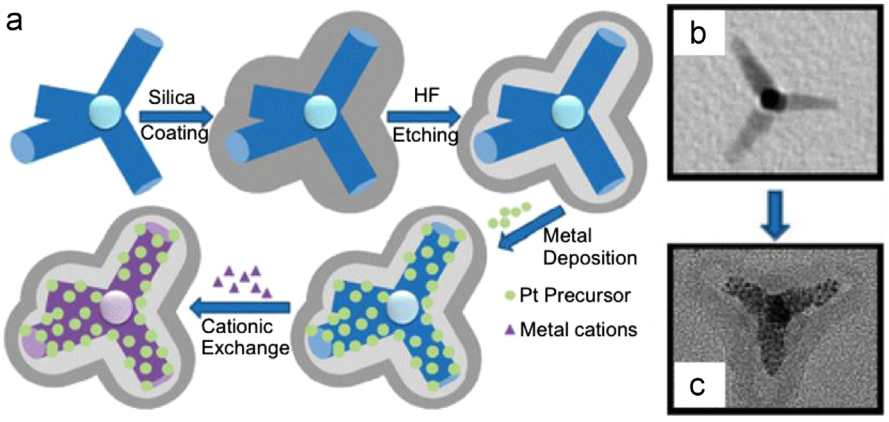


**Fig.7** Addition of selective dissolution to the method of "multistep sequential nucleation and growth" to increase the diversity and complexity orders of 3D complex structures. (a) Schematic representation of the stepwise growth of complex metal-semiconductor heterostructure through five steps; (b–c) TEM images of the starting CdSe tetrapod (b) and Pt-nanoparticle-decorated PtS nanotetrapods within a hollow $SiO_2$ interior (c). Reproduced with permission from J. Am. Chem. Soc., 134(21) (2012) 8754–8757.

work is very inspiring since it shows that nanocomponents can be assembled in a similar way as those molecular building units have been assembled to afford metal-organic-frameworks (MOFs) with many kinds of complex structures [125]. This direction should be paid much attention in later syntheses of nanostructured 3D complexes.

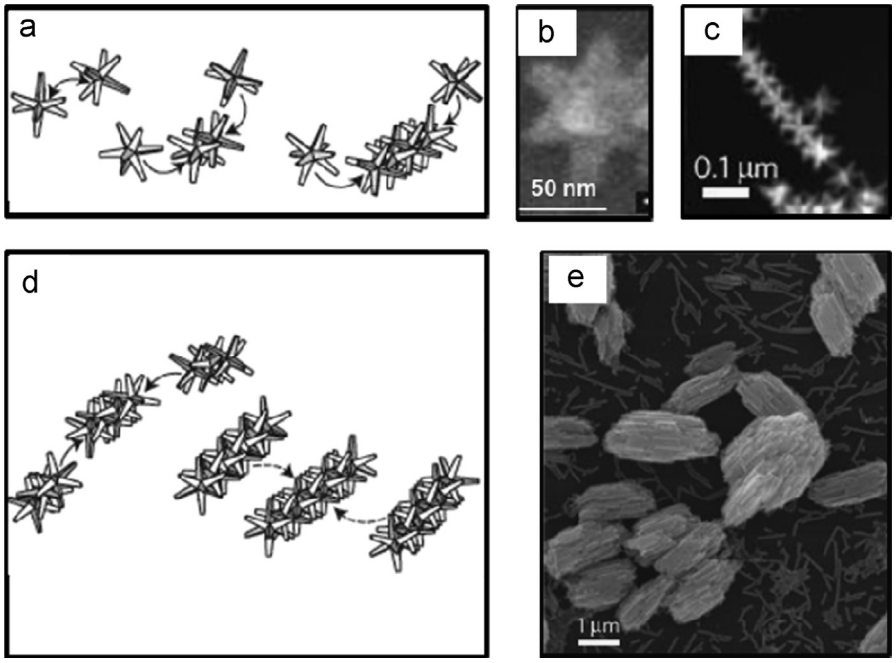


**Fig. 8** 3D hierarchical structures prepared from self-assembly of CdSe octapods. (a) Schematic representation of the assembly of CdSe octapods (b, TEM image) into 1D chain (c, SEM image); (d) Schematic representation of the assembly of 1D chains into 3D clusters (e, SEM image). (b) Reproduced with permission from Nano Lett. 10(9) (2010) 3770–3776; and others from Nature Mater. 10 (2011) 872–876.

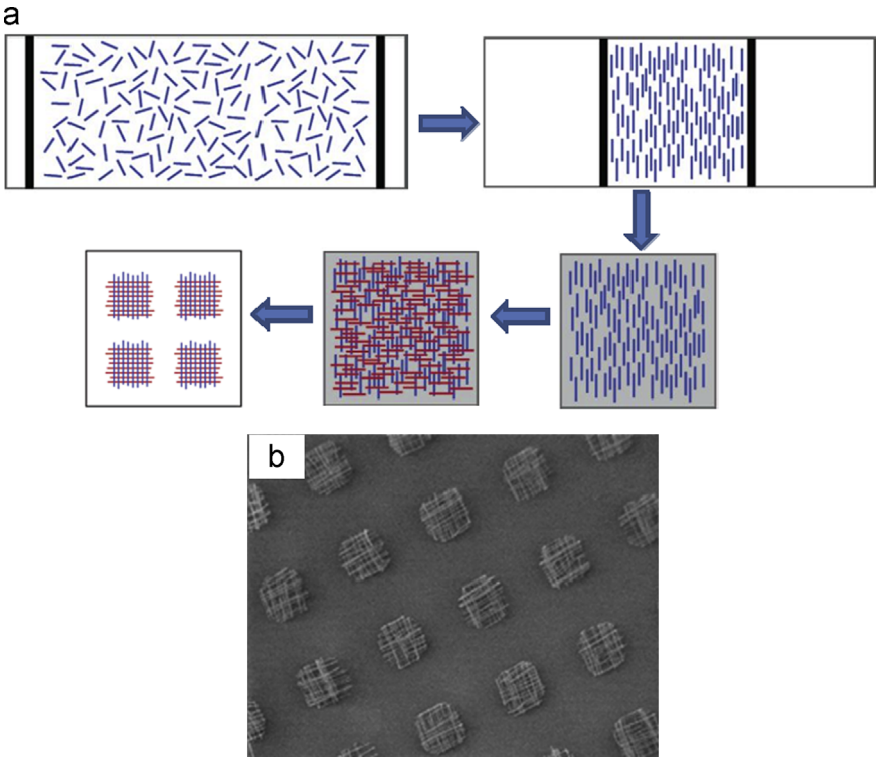


**Fig. 9** Large scale integration of arrays of crossed nanowires through the combination of Langmuir–Blodgett technique and photolithography. (a) Schematic representation of the stepwise assembly of 1D nanowires into 3D arrays of crossed nanowires; (b) SEM image of patterned arrays of crossed nanowires. Reproduced with permission from Nano Lett. 3(9) (2003) 1255–1259.

Scientists have also tried other kinds of methods to assemble nanocomponents into 3D complex structures. For example, the Langmuir–Blodgett (LB) technique [126] was used to organize inorganic nanorods into 2D and 3D assemblies [127] and prepare large area nanowire masks for deposition and etching [128]. Whang et al. further combined LB technique and photolithography

to organize nanowires into arrays of crossed nanowires/nanotubes structures over large areas (Fig. 9) [129]. A nanowire-surfactant monolayer (blue lines) on an aqueous subphase was compressed on a Langmuir–Blodgett trough to a specified pitch (Fig. 9a). The aligned nanowires were then transferred to the surface of a substrate to afford a uniform parallel array upon which a second layer of aligned parallel nanowire array (red lines) was put perpendicular to the first layer, resulting in the formation of crossed nanowires structures. If combined with photolithography, the two layers of nanowires could be arranged orthogonally to afford patterned arrays of crossed nanowires arrays (Fig. 9b). Electric-field was used to induce the formation of crossed nanowire arrays with lower complexities [130], showing its potential in organizing simple nanowires into 3D complexes especially if combined with other methods.

## 6. Nanostructured 3D complexes from template-assisted nanogrowths

Another important strategy to prepare nanostructured 3D complexes is template-assisted growth and the template could be soft or hard. Soft templates have been used to prepare many kinds of 3D complexes of semiconductors [131,132]. Conventional hard templates such as mesoporous silica templates with uniform pores have been used to successfully prepare 3D complexes of semiconductors [133,134]. In order to increase the complexity of the assembled 3D structures and enhance their functionalities, Rauber et al. developed a direct synthesis of highly ordered large-area nanowire networks assisted by hard templates [135]. Fig. 10a illustrates the scheme of the template fabrication and formation of a 3D complex nanowire network. A polycarbonate membrane was first irradiated by Au and U ions in several steps from different directions in a designed way as indicated by the angles ($\alpha$) and then etched by aqueous NaOH solution, resulting in the formation of a 3D network of cylindrical nanochannels. Then CdTe nanowires were filled up the nanochannels through electrodeposition. Subsequent removal of the polymer matrix afforded a freestanding 3D CdTe nanowire network (Fig. 10b) that demonstrate excellent electrical transport properties and efficient access of reactants to catalytic centers due to their porosity. This newly developed method allows good control of various parameters such as size, shape, chemical composition, orientation, and complexity of the macroscopically stable nanowire networks.

## 7. Summary and outlook

In summary, we have discussed recent progresses in multistep solution syntheses of nanostructured 3D complexes with fascinating morphologies. The structures are classified by the different combinations of nanocomponents with different dimensionalities, the orders of the topological complexities of the final structures, and synthetic methods. 1D nanocomponents have been found to be most frequently used either as backbones, grafting materials, or basic building units for assembly methods. The use of 2D and 3D nanocomponents for further growths and assembly methods could help grow nanostructured 3D complexes with higher orders of topological complexity. And most of the structures reported so far contain one or two chemical compositions and most of them are secondary or tertiary structures. Nanostructured 3D complexes containing more chemical compositions and having higher orders of topological complexity should be pursued since they might demonstrate better or even unprecedented functionalities. All the synthetic methods could be combined in different ways and new synthetic methods should be developed.

For all the proposed future research directions, the syntheses of nanostructured 3D complexes should be functionality-driven so that these 3D complex structures could find technological applications, which is crucial to the success of nanoscience and nanotechnology. For doing so, scientists and engineers need to pin down the exact growth mechanisms of many reported structures. They also need to correlate structures and functionalities, which is a daunting task since many factors such as overall topologies, organizations and orientations of nanocomponents, synergistic effects from different nanocomponents, surface states, junctions, etc. all play important roles in affecting the functionalities. System-level planning of experimental efforts and theoretical modeling [136] should help scientists and engineers understand the structure–functionality correlations and predict, design, and prepare structures with higher orders of topological complexity and improved/new functionalities.

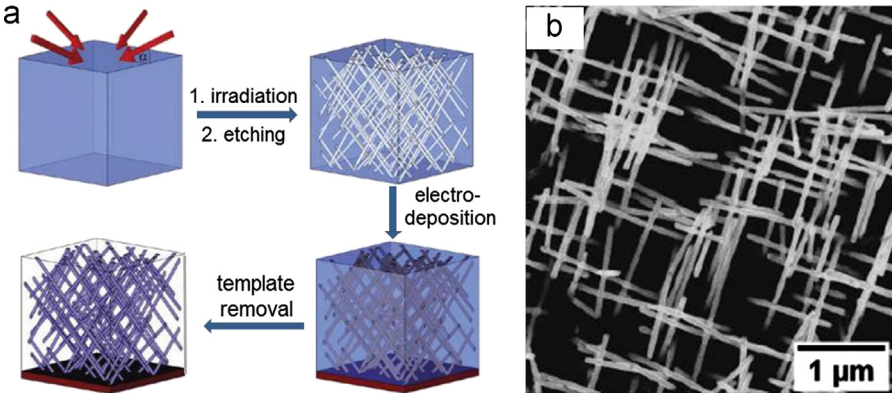


**Fig. 10** A 3D complex nanowire network with designed patterns prepared from template-assisted growth. (a) Schematic representation of the template fabrication and formation of the complex network; (b) SEM of a CdTe nanowire network. Reproduced with permission from Nano Lett. 11(6) (2011) 2304–2310.

## Acknowledgment

This work was partially supported by ABI and NSF through EPSCoR and MRSEC programs.

## References

[1] M.H. Huang, S. Mao, H. Feick, et al., Room-temperature ultraviolet nanowire nanolasers, Science 292 (5523) (2001) 1897–1899.
[2] X.F. Duan, C. Niu, V. Sahi, et al., High-performance thin-film transistors using semiconductor nanowires and nanoribbons, Nature 425 (2003) 274–278.
[3] B. Polyakov, B. Daly, J. Prikulis, et al., High-density arrays of germanium nanowire photoresistors, Advanced Materials 18 (14) (2006) 1812–1816.
[4] X.B. Chen, S.H. Shen, L.J. Guo, et al., Semiconductor-based photocatalytic hydrogen generation, Chemical Reviews 110 (11) (2010) 6503–6570.
[5] M. Grätzel, Photoelectrochemical cells, Nature 414 (2001) 338–344.
[6] F. Favier, E.C. Walter, M.P. Zach, et al., Hydrogen sensors and switches from electrodeposited palladium mesowire arrays, Science 293 (5538) (2001) 2227–2231.
[7] B.J. Hinds, N. Chopra, T. Rantell, et al., Aligned multiwalled carbon nanotube membranes, Science 303 (5654) (2004) 62–65.
[8] M.J. Bierman, S. Jin, Potential applications of hierarchical branching nanowires in solar energy, Energy and Environmental Science 2 (10) (2009) 1050–1059.
[9] W.L. Zhou, Z.L. Wang, Three-Dimensional Nanoarchitectures: Designing Next-Generation Devices, Springer, New York, 2011.
[10] D. Wang, C.M. Lieber, Nanocrystals branch out, Nature Materials 2 (2003) 355–356.
[11] L. Manna, D.J. Milliron, A. Meisei, et al., Controlled growth of tetrapod-branched inorganic nanocrystal, Nature Materials 2 (2003) 382–385.
[12] A.W. Smith, A. Rohatgi, Ray tracing analysis of the inverted pyramid texturing geometry for high efficiency silicon solar cells, Solar Energy Materials and Solar Cells 29 (1) (1993) 37–49.
[13] A.W. Blakers, A.H. Wang, A.M. Milne, et al., 22.8% efficient silicon solar cell, Applied Physics Letters 55 (13) (1989) 1363–1365.
[14] D.J. Milliron, I. Gur, A.P. Alivisatos, Hybrid organic-nanocrystal solar cells, MRS Bulletin 30 (01) (2005) 41–44.
[15] N.S. Lewis, Toward cost-effective solar energy use, Science 315 (5813) (2007) 798–801.
[16] Y.W. Cheng, S.T. Lu, H.B. Zhang, et al., Synergistic effects from graphene and carbon nanotubes enable flexible and robust electrodes for high-performance supercapacitors, Nano Letters 12 (8) (2012) 4206–4211.
[17] J. Hensel, G.M. Wang, Y. Li, et al., Synergistic effect of CdSe quantum dot sensitization and nitrogen doping of $TiO_2$ nanostructures for photoelectrochemical solar hydrogen generation, Nano Letters 10 (2) (2010) 478–483.
[18] K. Hata, D.N. Futaba, K. Mizuno, et al., Water-assisted highly efficient synthesis of impurity-free single-walled carbon nanotubes, Science 306 (5700) (2004) 1362–1364.
[19] J.Y. Lao, J.G. Wen, Z.F. Ren, Hierarchical ZnO nanostructures, Nano Letters 2 (11) (2002) 1287–1291.
[20] Z.W. Pan, Z.R. Dai, Z.L. Wang, Nanobelts of semiconducting oxides, Science 291 (5510) (2001) 1947–1949.
[21] J.B. Hannon, S. Kodambaka, F.M. Ross, et al., The influence of the surface migration of gold on the growth of silicon nanowires, Nature 440 (2006) 69–71.
[22] Z.I. Alferov, The history and future of semiconductor heterostructures, Semiconductors 32 (1) (1998) 1–14.
[23] J.H. Lee, Gas sensors using hierarchical and hollow oxide nanostructures: overview, Sensors and Actuators B: Chemical 140 (2009) 319–336.
[24] P.X. Gao, Metal Oxide Nanostructures and Their Applications, in: A. Umar (Ed.), American Scientific Publisher: Stevenson Ranch, CA, USA, 2010, pp. 513–545.
[25] D.J. Milliron, S.M. Hughes, Y. Cui, et al., Colloidal nanocrystal heterostructures with linear and branched topology, Nature 430 (2004) 190–195.
[26] L. Carbone, S. Kudera, E. Carlino, et al., Multiple wurtzite twinning in CdTe nanocrystals induced by methylphosphonic acid, Journal of the American Chemical Society 128 (3) (2006) 748–755.
[27] Y.W. Jun, Y.Y. Jung, J.W. Cheon, Architectural control of magnetic semiconductor nanocrystals, Journal of the American Chemical Society 124 (4) (2002) 615–619.
[28] Y.Y. Ma, Z.Y. Jiang, Q. Kuang, et al., Twin-crystal nature of the single-crystal-like branched $Cu_2O$ particles, Journal of Physical Chemistry C 112 (35) (2008) 13405–13409.
[29] Y.S. Ding, X.F. Shen, S. Gomez, et al., Hydrothermal growth of manganese dioxide into three-dimensional hierarchical nanoarchitectures, Advanced Functional Materials 16 (4) (2006) 549–555.
[30] F.R. Fan, Y. Ding, D.Y. Liu, et al., Facet-selective epitaxial growth of heterogeneous nanostructures of semiconductor and metal: ZnO nanorods on Ag nanocrystals, Journal of the American Chemical Society 131 (34) (2009) 12036–12037.
[31] K.T. Yong, Y. Sahoo, K.R. Choudhury, et al., Shape control of PbSe nanocrystals using noble metal seed particles, Nano Letters 6 (4) (2006) 709–714.
[32] S. Deka, A. Genovese, Z. Yang, et al., Phosphine-free synthesis of p-type copper(I) selenide nanocrystals in hot coordinating solvents, Journal of the American Chemical Society 132 (26) (2010) 8912–8914.
[33] S. Deka, K. Miszta, D. Dorfs, et al., Octapod-shaped colloidal nanocrystals of cadmium chalcogenides via one-pot cation exchange and seeded growth, Nano Letters 10 (9) (2010) 3770–3776.
[34] W. Wang, B.H. Gu, L. Liang, et al., Fabrication of near-infrared photonic crystals using N49 Technical note highly-monodispersed submicrometer $SiO_2$ spheres, Journal of Physical Chemistry B 107 (44) (2003) 12113–12117.
[35] T.R. Zhang, W.J. Dong, J. Kasbohm, et al., Design and hierarchical synthesis of branched heteromicrostructures, Smart Materials and Structures 15 (2) (2006) N46–N50.
[36] S. Srinivasan, A.K. Datye, M.H. Smith, et al., Interaction of titanium isopropoxide with surface hydroxyls on silica, Journal of Catalysis 145 (2) (1994) 565–573.
[37] T. Sugimoto, E. Matjević, Formation of uniform spherical magnetite particles by crystallization from ferrous hydroxide gels, Journal of Colloid and Interface Science 74 (1) (1980) 227–243.
[38] W. Stöber, A. Fink, E. Bohn, Controlled growth of monodisperse silica spheres in the micron size range, Journal of Colloid and Interface Science 26 (1) (1968) 62–69.
[39] U.K. Gautama, M. Imuraa, C.S. Routb, et al., Unipolar assembly of zinc oxide rods manifesting polarity-driven collective luminescence, Proceedings of the National Academy of Sciences of the USA 107 (31) (2010) 13588–13592.
[40] S.S. Mali, C.A. Betty, P.N. Bhosale, et al., Hydrothermal synthesis of rutile $TiO_2$ nanoflowers using Brønsted Acidic Ionic Liquid [BAIL]: synthesis, characterization and growth mechanism, CrystEngComm 14 (6) (2012) 1920–1924.
[41] S.Y. Zeng, K.B. Tang, T.W. Li, et al., Facile route for the fabrication of porous hematite nanoflowers: its synthesis, growth mechanism, application in the lithium ion battery, and magnetic and photocatalytic properties, Journal of Physical Chemistry 112 (13) (2008) 4836–4843.
[42] L.P. Qin, J.Q. Xu, X.W. Dong, et al., The template-free synthesis of square-shaped $SnO_2$ nanowires: the temperature effect and acetone gas sensors, Nanotechnology 19 (18) (2008) 185705.
[43] G. Cheng, K. Wu, P.T. Zhao, et al., Controlled growth of oxygen-deficient tin oxide nanostructures via a solvothermal approach in mixed solvents and their optical properties, Nanotechnology 18 (35) (2007) 355604.

[44] H.J. Zhang, R.F. Wu, Z.W. Chen, et al., Self-assembly fabrication of 3D flower-like ZnO hierarchical nanostructures and their gas sensing properties, CrysEngComm 14 (5) (2012) 1775–1782.
[45] M. Li, Y. Liu, H. Shen, Synthesis and characterization of large-scale hierarchical CdS microflowers, Chalcogenide Letters 8 (9) (2011) 555–560.
[46] W.T. Yao, S.H. Yu, S.J. Liu, et al., Architectural control syntheses of CdS and CdSe nanoflowers, branched nanowires, and nanotrees via a solvothermal approach in a mixed solution and their photocatalytic property, Journal of Physical Chemistry B 110 (24) (2006) 11704–11710.
[47] A.G. Kanaras, C. Sönnichsen, H.T. Liu, et al., Controlled synthesis of hyperbranched inorganic nanocrystals with rich three-dimensional structures, Nano Letters 5 (11) (2005) 2164–2167.
[48] P.M. Rørvik, T. Grande, M.A. Einarsrud, Hierarchial $PbTiO_3$ nanostructures grown on $SrTiO_3$ substrates, Crystal Growth and Design 9 (4) (2009) 1979–1984.
[49] C.H. Han, Y.Q. Pi, Q.Y. An, et al., Substrate-assisted self-organization of radial β-$AgVO_3$ nanowire clusters for high rate rechargeable lithium batteries, Nano Letters 12 (9) (2012) 4668–4673.
[50] L.L. Wang, T. Fei, Z. Lou, et al., Three-dimensional hierarchical flowerlike α-$Fe_2O_3$ nanostructures: synthesis and ethanol-sensing properties, ACS Applied Materials and Interfaces 3 (12) (2011) 4689–4694.
[51] K.M. AbouZeid, M.B. Mohamed, M.S. El-Shall, Hybrid Au–CdSe and Ag–CdSe nanoflowers and core–shell nanocrystals via one-pot heterogeneous nucleation and growth, Small 7 (23) (2011) 3299–3307.
[52] C. Cheng, Y.T. Shi, C. Zhu, et al., ZnO hierarchical structures for efficient quasi-solid dye-sensitized solar cells, Physical Chemistry Chemical Physics 13 (22) (2011) 10631–10634.
[53] D. Keyson, D.P. Volanti, L.S. Cavalcante, et al., CuO urchin-nanostructures synthesized from a domestic hydrothermal microwave method, Materials Research Bulletin 43 (3) (2008) 771–775.
[54] X.Y. Zeng, J.L. Yuan, Z.Y. Wang, et al., Nanosheet-based microspheres of Eu3+-doped ZnO with efficient energy transfer from ZnO to $Eu^{3+}$ at room temperature, Advanced Materials 19 (24) (2007) 4510–4514.
[55] M. Mo, J.C. Yu, L. Zhang, et al., Self-assembly of ZnO nanorods and nanosheets into hollow microhemispheres and microspheres, Advanced Materials 17 (6) (2005) 756–760.
[56] Z. Ren, Y.B. Guo, G. Wrobel, et al., Three dimensional koosh ball nanoarchitecture with a tunable magnetic core, fluorescent nanowire shell and enhanced photocatalytic property, Journal of Materials Chemistry 22 (14) (2012) 6862–6868.
[57] C. Lévy-Clément, X.D. Wang, C. Benoit-Moez, et al., Applications of colloidal crystal patterning for synthesis of 1D and 3D nanostructured semiconductors, Physics Status Solidi A 208 (6) (2011) 1426–1432.
[58] P. Jiang, J.J. Zhou, H.F. Fang, et al., Hierarchical shelled ZnO structures made of bunched nanowire arrays, Advanced Functional Materials 17 (8) (2007) 1303–1310.
[59] D. Barpuzary, Z. Khan, N. Vinothkumar, et al., Hierarchically grown urchinlike CdS@ZnO and CdS@$Al_2O_3$ heteroarrays for efficient visible-light-driven photocatalytic hydrogen generation, Journal of Physical Chemistry C 116 (1) (2012) 150–156.
[60] W.D. Zhang, Growth of ZnO nanowires on modified well-aligned carbon nanotube arrays, Nanotechnology 17 (4) (2006) 1036–1040.
[61] W.D. Zhang, Y. Wen, S.M. Liu, et al., Synthesis of vertically aligned carbon nanotubes on metal deposited quartz plates, Carbon 40 (11) (2002) 1981–1989.
[62] N. Fu, Z. Li, A. Myalitsin, et al., One-dimensional heterostructures of single-walled carbon nanotubes and CdSe nanowires, Small 6 (3) (2010) 376–380.
[63] D.F. Zhang, L.D. Sun, C.J. Jia, et al., Hierarchical assembly of $SnO_2$ nanorod arrays on α-$Fe_2O_3$ nanotubes: a case of interfacial lattice compatibility, Journal of the American Chemical Society 127 (39) (2005) 13492–13493.
[64] M.S. Mo, S.H. Lim, Y.W. Ma, et al., In situ self-assembly of thin ZnO nanoplatelets into hierarchical mesocrystal microtubules with surface grafting of nanorods: a general strategy towards hollow mesocrystal structures, Advanced Materials 20 (2) (2008) 339–342.
[65] P. Sudhagar, T. Song, D.H. Lee, et al., High open circuit voltage quantum dot sensitized solar cells manufactured with ZnO nanowire arrays and Si/ZnO branched hierarchical structures, Journal of Physical Chemistry Letters 2 (16) (2011) 1984–1990.
[66] K. Sun, Y. Jing, N. Park, et al., Solution synthesis of large-scale, high-sensitivity ZnO/Si hierarchical nanoheterostructure photodetectors, Journal of the American Chemical Society 132 (44) (2010) 15465–15467.
[67] K. Sun, Y. Jing, C. Li, et al., 3D branched nanowire heterojunction photoelectrodes for high-efficiency solar water splitting and $H_2$ generation, Nanoscale 4 (5) (2012) 1515–1521.
[68] S. Haller, T. Suguira, D. Lincot, et al., Design of a hierarchical structure of ZnO by electrochemistry for ZnO-based dye-sensitized solar cells, Physica Status Solidi A 207 (10) (2010) 2252–2257.
[69] H.M. Cheng, W.H. Chiu, C.H. Lee, et al., Formation of branched ZnO nanowires from solvothermal method and dye-sensitized solar cells applications, Journal of Physical Chemistry C 112 (42) (2008) 16359–16364.
[70] Y.F. Zhu, G.H. Zhou, H.Y. Ding, et al., Synthesis of highly-ordered hierarchical ZnO nanostructures and their application in dye-sensitized solar cells, Crystal Research and Technology 45 (10) (2010) 1075–1078.
[71] C.H. Wang, C.L. Shao, X.T. Zhang, et al., $SnO_2$ nanostructures-$TiO_2$ nanofibers heterostructures: controlled fabrication and high photocatalytic properties, Inorganic Chemistry 48 (15) (2009) 7261–7268.
[72] N.X. Wang, C.H. Sun, Y. Zhao, et al., Fabrication of three-dimensional ZnO/$TiO_2$ heteroarchitectures via a solution process, Journal of Materials Chemistry 18 (33) (2008) 3909–3911.
[73] Q.J. Zhang, C.H. Sun, J. Yan, et al., Perpendicular rutile nanosheets on anatase nanofibers: heterostructured $TiO_2$ nanocomposites via a mild solvothermal method, Solid State Sciences 12 (7) (2010) 1274–1277.
[74] M. Shang, W.Z. Wang, W.Z. Yin, et al., General strategy for a large-scale fabric with branched nanofiber–nanorod hierarchical heterostructure: controllable synthesis and applications, Chemistry—A European Journal 16 (37) (2010) 11412–11419.
[75] H.G. Yang, H.C. Zeng, Synthetic architectures of $TiO_2$/$H_2Ti_5O_{11} \cdot H_2O$, ZnO/$H_2Ti_5O_{11} \cdot H_2O$, ZnO/$TiO_2$/$H_2Ti_5O_{11} \cdot H_2O$, and ZnO/$TiO_2$ nanocomposites, Journal of the American Chemical Society 127 (1) (2005) 270–278.
[76] J.K. Oh, J.K. Lee, H.S. Kim, et al., $TiO_2$ branched nanostructure electrodes synthesized by seeding method for dye-sensitized solar cells, Chemical Materials 22 (3) (2010) 1114–1118.
[77] C.W. Cheng, B. Liu, H.Y. Yang, et al., Hierarchical assembly of ZnO nanostructures on $SnO_2$ backbone nanowires: low-temperature hydrothermal preparation and optical properties, ACS Nano 3 (10) (2009) 3069–3076.
[78] M.T. Niu, F. Huang, L.F. Cui, et al., Hydrothermal synthesis, structural characteristics, and enhanced photocatalysis of $SnO_2$/α-$Fe_2O_3$ semiconductor nanoheterostructures, ACS Nano 4 (2) (2010) 681–688.
[79] H.J. Kim, S.H. Jeon, M.Y. Lee, et al., Fabrication of a novel hierarchical assembly of ZnO nanowires on WOx nanowhiskers for highly efficient field electron emission, Journal of Materials Chemistry 21 (35) (2011) 13458–13463.
[80] H.J. Kim, M.S. Seol, J.H. Lee, et al., Highly efficient photoelectrochemical hydrogen generation using hierarchical ZnO/WOx nanowires cosensitized with CdSe/CdS, Journal of Physical Chemistry C 115 (51) (2011) 25429–25436.
[81] T.L. Sounart, J. Liu, J.A. Voigt, et al., Secondary nucleation and growth of ZnO, Journal of the American Chemical Society 129 (51) (2007) 15786–15793.
[82] T.R. Zhang, W.J. Dong, M. Keeter-Brewer, et al., Site-specific nucleation and growth kinetics in hierarchical nanosyntheses of

branched ZnO crystallites, Journal of the American Chemical Society 128 (33) (2006) 10960–10968.
[83] X.C. Jianga, B.Z. Tian, J. Xianga, et al., Rational growth of branched nanowire heterostructures with synthetically encoded properties and function, Proceedings of the National Academy of Sciences of the USA 108 (30) (2011) 12212–12216.
[84] C.D. Gu, C. Cheng, H.Y. Huang, et al., Growth and photocatalytic activity of dendrite-like ZnO@Ag heterostructure nanocrystals, Crystal Growth and Design 9 (7) (2009) 3278–3285.
[85] P. Zhang, C. Shao, M. Zhang, et al., $Bi_2MoO_6$ ultrathin nanosheets on $ZnTiO_3$ nanofibers: a 3D open hierarchical heterostructures synergistic system with enhanced visible-light-driven photocatalytic activity, Journal of Hazardous Materials (217–218) (2012) 422–428.
[86] L.Q. Mai, F. Yang, Y.L. Zhao, et al., Hierarchical $MnMoO_4$/$CoMoO_4$ heterostructured nanowires with enhanced supercapacitor performance, Nature Communications 2 (2012) 381.
[87] L. Yang, S. Cheng, Y. Ding, et al., Hierarchical network architectures of carbon fiber paper supported cobalt oxide nanonet for high-capacity pseudocapacitors, Nano Letters 12 (1) (2012) 321–325.
[88] Y. Qin, X.D. Wang, Z.L. Wang, Microfibre–nanowire hybrid structure for energy scavenging, Nature 451 (2008) 809–813.
[89] B. Weintraub, Y.G. Wei, Z.L. Wang, Optical fiber/nanowire hybrid structures for efficient three-dimensional dye-sensitized solar cells, Angewandte Chemie International Edition 48 (47) (2009) 8981–8985.
[90] A. Mohanty, N. Garg, R.C. Jin, A universal approach to the synthesis of noble metal nanodendrites and their catalytic properties, Angewandte Chemie International Edition 49 (29) (2010) 4962–4966.
[91] V. Polshettiwar, B. Baruwati, R.S. Varma, Self-assembly of metal oxides intothree-dimensional nanostructures: synthesis and application in catalysis, ACS Nano 3 (3) (2009) 728–736.
[92] K. Drozdowicz-Tomsia, F. Xie, E.M. Goldys, Deposition of silver dentritic nanostructures on silicon for enhanced fluorescence, Journal of Physical Chemistry C 114 (3) (2010) 1562–1569.
[93] X.G. Wen, Y.T. Xie, M.W. Cheung, et al., Dendritic nanostructures of silver: facile synthesis, structural characterizations, and sensing applications, Langmuir 22 (10) (2006) 4836–4842.
[94] P. Zhou, Z.H. Dai, M. Fang, et al., Novel dendritic palladium nanostructure and its application in biosensing, Journal of Physical Chemistry C 111 (34) (2007) 12609–12616.
[95] P. Galenko, V. Zhuravlev, Physics of Dendrites: Computational Experiments, World Scientific, Singapore, 1994.
[96] D. Kuang, A. Xu, Y. Fang, et al., Surfactant-assisted growth of novel PbS dendritic nanostructures via facile hydrothermal process, Advanced Materials 15 (20) (2003) 1747–1750.
[97] C.M. McShane, K.S. Choi, Photocurrent enhancement of n-type $Cu_2O$ electrodes achieved by controlling dendritic branching growth, Journal of the American Chemical Society 131 (7) (2009) 2561–2569.
[98] A.G Dong, R. Tang, W.E. Buhro, Solution-based growth and structural characterization of homo- and heterobranched semiconductor nanowires, Journal of the American Chemical Society 129 (40) (2007) 12254–12262.
[99] Q.T. Pan, K. Huang, S.B. Ni, et al., Synthesis of α-$Fe_2O_3$ dendrites by a hydrothermal approach and their application in lithium-ion batteries, Journal of Physics D Applied Physics 42 (2009) 015417.
[100] G.B. Sun, B.X. Dong, M.H. Cao, et al., Hierarchical dendrite-like magnetic materials of $Fe_3O_4$, γ-$Fe_2O_3$, and Fe with high performance of microwave absorption, Chemical Materials 23 (6) (2011) 1587–1593.
[101] S.H. Ko, D. Lee, H.W. Kang, et al., Nanoforest of hydrothermally grown hierarchical ZnO nanowires for a high efficiency dye-sensitized solar cell, Nano Letters 11 (2) (2011) 666–671.
[102] C.T. Wu, J.J. Wu, Room-temperature synthesis of hierarchical nanostructures on ZnO nanowire anodes for dye-sensitized solar cells, Journal of Materials Chemistry 21 (35) (2011) 13605–13610.
[103] M. McCune, W. Zhang, Y. Deng, A 3D ZnO nanowire-based dye-sensitized solar cell (DSSC) with unique caterpillar-like structure, Nano Letters 12 (7) (2012) 3656–3662.
[104] F.H. Zhao, J.G. Zheng, X.F. Yang, et al., Complex ZnO nanotree arrays with tunable top, stem and branch structures, Nanoscale 2 (9) (2010) 1674–1683.
[105] I.S. Cho, Z. Chen, A.J. Forman, et al., Branched $TiO_2$ nanorods for photoelectrochemical hydrogen production, Nano Letters 11 (11) (2011) 4978–4984.
[106] J.Y. Liao, B.X. Lei, H.Y. Chen, et al., Oriented hierarchical single crystalline anatase $TiO_2$ nanowire arrays on Ti-foil substrate for efficient flexible dye-sensitized solar cells, Energy and Environmental Sciences 5 (2) (2012) 5750–5757.
[107] F. Shao, J. Sun, L. Gao, et al., Forest-like $TiO_2$ hierarchical structures for efficient dye-sensitized solar cells, Journal of Materials Chemistry 22 (14) (2012) 6824–6830.
[108] M.H. Cao, T.F. Liu, S. Gao, et al., Single-crystal dendritic micropines of magnetic α-$Fe_2O_3$: large-scale synthesis, formation mechanism, and properties, Angewandte Chemie International Editions 44 (27) (2005) 4197–4201.
[109] Q.Y. Lu, F. Gao, S. Komarneni, Biomolecule-assisted synthesis of highly ordered snowflakelike structures of bismuth sulfide nanorods, Journal of the American Chemical Society 126 (1) (2004) 54–55.
[110] G.J. Zhou, M.K. Lu, Z.L. Xiu, et al., Controlled synthesis of high-quality PbS star-shaped dendrites, multipods, truncated nanocubes, and nanocubes and their shape evolution process, Journal of Physical Chemistry B 110 (13) (2006) 6543–6548.
[111] S.H.De Paoli Lacerda, J.F. Douglas, S.D. Hudson, et al., Quantum mazes: luminescent labyrinthine semiconductor nanocrystals having a narrow emission spectrum, ACS Nano 1 (4) (2007) 337–347.
[112] F. Xu, M. Dai, Yi.N. Lu, et al., Hierarchical ZnO nanowire −nanosheet architectures for high power conversion efficiency in dye-sensitized solar cells, Journal of Physical Chemistry C 114 (6) (2010) 2776–2782.
[113] L.F. Xu, Q.W. Chen, D.S. Xu, Hierarchical ZnO nanostructures obtained by electrodeposition, Journal of Physical Chemistry C 111 (31) (2007) 11560–11565.
[114] J.H. Qiu, M. Guo, X.D. Wang, Electrodeposition of hierarchical ZnO nanorod-nanosheet structures and their applications in dye-sensitized solar cells, ACS Applied Materials Interfaces 3 (7) (2011) 2358–2367.
[115] W.W. Zhou, Y.Y. Tay, X.T. Jia, et al., Controlled growth of $SnO_2$@$Fe_2O_3$ double-sided nanocombs as anodes for lithium-ion batteries, Nanoscale 4 (15) (2012) 4459–4463.
[116] Y.C. Qiu, K.Y. Yan, H. Deng, et al., Secondary branching and nitrogen doping of ZnO nanotetrapods: building a highly active network for photoelectrochemical water splitting, Nano Letters 12 (1) (2012) 407–413.
[117] T.L. Sounart, J. Liu, J.A. Voigt, et al., Sequential nucleation and growth of complex nanostructured films, Advanced Functional Materials 16 (3) (2006) 335–344.
[118] Z.R. Tian, J.A. Voigt, J. Liu, et al., Complex and oriented ZnO nanostructures, Nature Materials 2 (2003) 821–826.
[119] P.C. Hidber, T.J. Graule, L.J. Gauckler, Citric acid—a dispersant for aqueous alumina suspensions, Journal of the American Ceramic Society 79 (7) (1996) 1857–1867.
[120] J. Lian, Y. Xu, M. Lin, et al., Aqueous-phase reactions on hollow silica-encapsulated semiconductor nanoheterostructures, Journal of the American Chemical Society 134 (21) (2012) 8754–8757.
[121] A. Fiore, R. Mastria, M.G. Lupo, et al., Tetrapod-shaped colloidal nanocrystals of II−VI semiconductors prepared by seeded growth, Journal of the American Chemical Society 131 (6) (2009) 2274–2282.
[122] T. Selvan, T.T. Tan, J.Y. Ying, Robust, non-cytotoxic, silica-coated CdSe quantum dots with efficient photoluminescence, Advanced Materials 17 (13) (2005) 1620–1625.
[123] Y.J. Wong, L. Zhu, W.S. Teo, et al., Revisiting the Stöber method: inhomogeneity in silica shells, Journal of the American Chemical Society 133 (30) (2011) 11422–11425.
[124] K. Miszta, J. de Graaf, G. Bertoni, et al., Hierarchical self-assembly of suspended branched colloidal nanocrystals into superlattice structures, Nature Materials 10 (2011) 872–876.

[125] M. Eddaoudi, D.B. Moler, H.L. Li, et al., Modular chemistry: secondary building units as a basis for the design of highly porous and robust metal-organic carboxylate frameworks, Accounts of Chemical Research 34 (4) (2001) 319–330.
[126] A. Ulman, An Introduction to Ultrathin Organic Films: From Langmuir–Blodgett to Self-assembly, Academic Press, New York, 1991.
[127] F. Kim, S. Kwan, J. Akana, et al., Langmuir–Blodgett nanorod assembly, Journal of the American Chemical Society 123 (18) (2001) 4360–4361.
[128] D. Whang, S. Jin, C.M. Lieber, Nanolithography using hierarchically assembled nanowire masks, Nano Letters 3 (7) (2003) 951–954.
[129] D. Whang, S. Jin, Y. Wu, et al., Large-scale hierarchical organization of nanowire arrays for integrated nanosystems, Nano Letters 3 (9) (2003) 1255–1259.
[130] Z.H. Zhong, D.L. Wang, Y. Cui, et al., Nanowire crossbar arrays as address decoders for integrated nanosystems, Science 302 (5649) (2003) 1377–1379.
[131] Y.S. Luo, S.Q. Li, Q.F. Ren, et al., Facile synthesis of flowerlike $Cu_2O$ nanoarchitectures by a solution phase route, Crystal Growth and Design 7 (1) (2007) 87–92.
[132] L. Zhang, N. Gaponik, J. Müller, et al., Branched wires of CdTe nanocrystals using amphiphilic molecules as templates, Small 1 (5) (2005) 524–527.
[133] D.H. Wang, H.M. Luo, R. Kou, et al., A general route to macroscopic hierarchical 3D nanowire networks, Angewandte Chemie International Edition 43 (45) (2004) 6169–6173.
[134] D.H. Wang, H.P. Jakobson, R. Kou, et al., Metal and semiconductor nanowire network thin films with hierarchical pore structures, Chemical Materials 18 (18) (2006) 4231–4237.
[135] M. Rauber, I. Alber, S. Muller, et al., Highly-ordered supportless three-dimensional nanowire networks with tunable complexity and interwire connectivity for device integration, Nano Letters 11 (6) (2011) 2304–2310.
[136] P.D Yang, J.M. Tarascon, Towards systems materials engineering, Nature Materials 11 (2012) 560–563.

**Z. Ryan** Tian received his PhD in Chemistry in 1997 from University of Connecticut, and then conducted postdoctoral research at the University of California, Davis and then the Sandia National Laboratories. Since 2004, he has been working at the University of Arkansas, and currently is an Associate Professor in Chemistry/Biochemistry, Institute of Nanoscience/Engineering, Cell/Molecular Biology, and Microelectronics/Photonics, and an adjunct faculty in the College of Engineering. One of his lab's thrust areas in research is to construct simple nanoscale building-blocks into complex crystallites, each possessing highly hierarchical and ordered spatial regularities with a confined three-dimensional space, typically in an oriented array on a large substrate. Thus-made nanocomplex materials can show collective and even spatially concerted function(s) of these building-blocks, precisely by design, for tackling longstanding problems in heterogeneous catalysis, energy storage and conversion, sensing, etc.